HYBRID TDIE-TDPO METHOD FOR STUDYING ON TRANSIENT RESPONSES OF SOME WIRE AND SURFACE STRUCTURES ILLUMINATED BY AN ELECTROMAGNETIC PULSE

W. Luo

Center for Microwave and RF Technologies
Key Lab of Educational Ministry for Design and EMC of High-Speed
Electronic Systems
Shanghai Jiao Tong University, Shanghai 200240, China

W.-Y. Yin [†]

Center for Optical and EM Research (COER), State Key Lab of MOI
Zhejiang University, Hangzhou 310058, China

M.-D. Zhu

Center for Microwave and RF Technologies
Key Lab of Educational Ministry for Design and EMC of High-Speed
Electronic Systems
Shanghai Jiao Tong University, Shanghai 200240, China

J.-Y. Zhao

Center for Optical and EM Research (COER), State Key Lab of MOI
Zhejiang University, Hangzhou 310058, China

Abstract—An efficient hybrid method, based on time-domain integral equation (TDIE) and time-domain physical optics (TDPO), is proposed for studying on transient electromagnetic responses of some wire and surface structures illuminated by an electromagnetic pulse (EMP), respectively. Two groups of triangular-type basis functions are used to expand the currents on both of them. The derived

hybrid TDIE-TDPO equations are solved by marching-on-in-time (MOT) scheme. In comparison with the full TDIE-based MOT method, computational complexity of our developed method is reduced significantly, and at the same time, with high accuracy maintained. Numerical results of EMP responses of some typical wire and surface structures are presented to demonstrate its versatility, accuracy and efficiency, with proximity effects between them captured and discussed.

1. INTRODUCTION

In the study of EMC and EMI problems of various communication systems, we often require wideband transient responses of many perfectly conducting objects with arbitrary geometries in the presence of one or more electromagnetic interference signals [1–10]. We know that time-domain electric field integral equation (TD-EFIE) technique [11–19] has been used for studying many scattering, radiation and signal transmission problems in the time domain. In order to solve the TD-EFIE, marching-on-in-time (MOT) scheme [20] is often implemented. However, MOT-based TDIE solver always suffers from high computational complexity. Its computational cost for large scale problems increases rapidly with operating frequency. To handle such a difficulty, we need to employ other methods, such as Physical Optics (PO), etc.. The PO method is accurate for studying electrically large and smooth objects. However, many electrically large ones often have fine structures which are very electrically small in comparison with single wavelength. Under such circumstances, hybrid method consisting of TDIE and time-domain PO (TDPO) will be an appropriate choice [21–26].

In this paper, an efficient hybrid method of TDIE-TDPO is successfully implemented for studying on transient electromagnetic responses of several wire and surface structures in the presence of an EMP. In our method, a group of planar triangular patches [27] are used to simulate the surface structure with the spatial RWG basis function employed, and a linear tubular segment model is used for simulating the wire structure with the triangular spatial basis function implemented [28]. Here, the temporal basis functions of the high order time domain ones are also employed in our mathematical treatment. In particular, each structure is partitioned into TDIE and TDPO regions. In the TDIE region, surface currents are updated by solving one TD-EFIE using the MOT scheme. While in the TDPO region, PO currents are obtained according to the incident fields as well as the ones radiated by all currents in the TDIE ones. Under such circumstances, using our proposed hybrid TDIE-TDPO method, computational complexity can

be reduced significantly. In contrast to the results obtained by TD-EFIE based on MOT scheme, our method is accurate and efficient for handling various transient scattering and radiating problems of composite structures, with proximity effects between them captured and examined in detail.

2. FORMULATION

As shown in Fig. 1, the parameter S denotes one perfectly conducting surface illuminated by an electromagnetic pulse, and $\mathbf{n}$ denotes the outward pointing normal to S. In general, it consists of one conducting object denoted by S_B and one or several conducting wires (S_W). So, we can divide the problem domain into TDIE and TDPO regions, denoted by S^{IE} and S^{PO}, respectively. The TDIE region consists of the full wire surface S_W and a part of the object surface S_B, and the remaining part of S_B is the TDPO one.
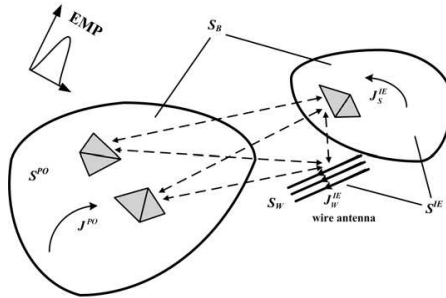

Figure 1. Geometry of the problem.

The incident EMP is described by $\{\mathbf{E}^i(\mathbf{r}, t), \mathbf{H}^i(\mathbf{r}, t)\}$, and its interaction with the surface S induces a surface current denoted by $\mathbf{J}(\mathbf{r}, t)$, which in turn generates the scattered fields $\{\mathbf{E}^S(\mathbf{r}, t), \mathbf{H}^S(\mathbf{r}, t)\}$, as described by

$$\mathbf{E}^S(\mathbf{J}(\mathbf{r}, t)) = -L(\mathbf{J}), \tag{1}$$

$$\mathbf{H}^S(\mathbf{J}(\mathbf{r}, t)) = K(\mathbf{J}), \tag{2}$$

$$L(\mathbf{J}) = \frac{\mu}{4\pi} \int_S \frac{1}{R} \frac{\partial}{\partial t} \mathbf{J}(\mathbf{r}, \tau) \, dS' + \frac{1}{4\pi\varepsilon} \nabla \int_S \frac{1}{R} \sigma(\mathbf{r}, \tau) \, dS'$$

$$= \frac{\mu}{4\pi} \int_S \frac{1}{R} \frac{\partial}{\partial t} \mathbf{J}(\mathbf{r}, \tau) \, dS' - \frac{1}{4\pi\varepsilon} \nabla \int_S \frac{1}{R} \int_{-\infty}^{\tau} \nabla' \cdot \mathbf{J}(\mathbf{r}, t') \, dt' dS', \quad (3)$$

$$K(\mathbf{J}) = \frac{1}{4\pi} \int_S \nabla \times \frac{\mathbf{J}(r,\tau)}{R} dS'. \tag{4}$$

where $R = |\mathbf{r} - \mathbf{r}'|$ represents the distance between an arbitrary observation point $\mathbf{r}$ and the source one $\mathbf{r}'$, $\tau = t - R/c$ is the retarded time, μ and ε are the permeability and the permittivity of the outer space of structure, in which the velocity of electromagnetic wave is denoted by c, σ is the surface charge density, and $\mathbf{J}$ is the surface current density of the structure.

By applying the boundary condition on the surface S, we obtain

$$\mathbf{n} \times \left[\mathbf{E}^S\left(\mathbf{J}^{IE}(\mathbf{r},t)\right) + \mathbf{E}^S\left(\mathbf{J}^{PO}(\mathbf{r},t)\right) + \mathbf{E}^i(\mathbf{r},t) \right] = 0, \quad \forall \mathbf{r} \in S^{IE} \tag{5}$$

$$\mathbf{J}^{PO}(\mathbf{r},t) = 2\hat{\mathbf{n}} \times \left[\mathbf{H}^s\left(\mathbf{J}^{IE}(\mathbf{r},t)\right) + \mathbf{H}^s\left(\mathbf{J}^{PO}(\mathbf{r},t)\right) + \mathbf{H}^i(\mathbf{r},t) \right], \quad \forall \mathbf{r} \in S^{PO} \tag{6}$$

In the TDIE region, the excited currents are updated by solving one TD-EFIE. In the TDPO one, currents are obtained using the TDPO approximation, which inherently neglects the mutual interaction effects within currents in the TDPO region and imposes the shadowed condition [23]. Thus, we obtain

$$\mathbf{E}^i(\mathbf{r},t)\big|_{\tan} = L\left(\mathbf{J}^{IE}\right) + L\left(\mathbf{J}^{PO}\right)\big|_{\tan}, \quad \forall \mathbf{r} \in S^{IE} \tag{7}$$

$$\mathbf{J}^{PO}(\mathbf{r},t) = 2\hat{\mathbf{n}} \times \mathbf{H}^i(\mathbf{r},t) + 2\hat{\mathbf{n}} \times K\left(\mathbf{J}^{IE}\right), \quad \forall \mathbf{r} \in S^{PO} \tag{8}$$

In order to handle the time integral term in (3) together with the time derivative of the vector potential, we introduce a new source vector $\mathbf{P}$, defined by

$$\mathbf{J}(\mathbf{r},t) = \frac{\partial}{\partial t} \mathbf{P}(\mathbf{r},t), \tag{9}$$

$$\sigma(\mathbf{r},t) = -\nabla' \cdot \mathbf{P}(\mathbf{r},t). \tag{10}$$

The vector potential $\mathbf{P}^{IE}$ and $\mathbf{P}^{PO}$ in both TDIE and TDPO regions are expanded individually using the spatial-temporal basis functions [20] as

$$\begin{aligned}
\mathbf{P}^{IE}(r',t) &= (4\pi\varepsilon_0) \sum_{i=1}^{N_t} \sum_{n=1}^{N^{IE}} P_{n,i}^{IE} \mathbf{f}_n^{IE}(\mathbf{r}') T(t - i\Delta t) \\
&= (4\pi\varepsilon_0) \sum_{i=1}^{N_t} \sum_{n=1}^{N_S^{IE}} P_{n,i}^{S} \mathbf{f}_n^{S}(\mathbf{r}') T(t - i\Delta t) \\
&\quad + (4\pi\varepsilon_0) \sum_{i=1}^{N_t} \sum_{n=1}^{N_W^{IE}} P_{n,i}^{W} \mathbf{f}_n^{W}(\mathbf{r}') T(t - i\Delta t),
\end{aligned} \tag{11}$$

and

$$\mathbf{P}^{PO}\left(\mathbf{r}',t\right) = (4\pi\varepsilon_0)\sum_{i=1}^{N_t}\sum_{n=1}^{N^{PO}} P_{n,i}^{PO}\mathbf{f}_n^{PO}\left(\mathbf{r}'\right)T\left(t-i\Delta t\right), \quad (12)$$

where $P_{n,i}^{IE}$ and $P_{n,i}^{PO}$ are the coefficients corresponding to the TDIE and TDPO regions, respectively. The variables $P_{n,i}^{S}$ and $P_{n,i}^{W}$ are the coefficients corresponding to the surface and wire parts, respectively, which all belong to the TDIE region. The parameters N^{IE}, N^{PO} and N_t are the spatial and temporal free degrees in both regions, respectively. The function $\mathbf{f}_n^S(\mathbf{r}')$ is the spatial basis one used for the TDIE region, while $\mathbf{f}_n^{PO}(\mathbf{r}')$ is used for the TDPO one. These basis functions are different from each other, but both are used for simulating the surface of the 3-D conductive objects. Therefore, a set of RWG basis functions is needed here. For an arbitrary wire structure, we use "reduced kernel" to approximate the wire part [28, 29], and $\mathbf{f}_n^W(\mathbf{r}')$ is chosen to be the piecewise triangular basis one. The variable Δt is the time step, and $T(t)$ is the high-order temporal basis function [19].

By expressing the terms $\mathbf{L}(\mathbf{P}^{IE})$, $\mathbf{L}(\mathbf{P}^{PO})$ and $\mathbf{K}(\mathbf{P}^{IE})$ in (7) and (8) as the integral forms of $\{\mathbf{P}^{IE}\left(\mathbf{r},t\right), \mathbf{P}^{PO}\left(\mathbf{r},t\right)\}$ in (11) and (12), and testing (7) and (8) using the separate functions $\mathbf{f}_m^S(\mathbf{r})$, $\mathbf{f}_m^W(\mathbf{r})$ and $\mathbf{f}_m^{PO}(\mathbf{r})$ at the time $t_j = j\Delta t$, a set of matrix equations is derived as follows:

$$\begin{bmatrix} Z_0^{S-S} & Z_0^{S-W} & Z_0^{S-PO} \\ Z_0^{W-S} & Z_0^{W-W} & Z_0^{W-PO} \\ Z_0^{PO-S} & Z_0^{PO-W} & C_0^{PO-PO} \end{bmatrix}\begin{bmatrix} P_j^S \\ P_j^W \\ P_j^{PO} \end{bmatrix}$$

$$=\begin{bmatrix} V_j^S \\ V_j^W \\ V_j^{PO} \end{bmatrix} - \sum_{i=1}^{\min(j,L)}\begin{bmatrix} Z_i^{S-S} & Z_i^{S-W} & Z_i^{S-PO} \\ Z_i^{W-S} & Z_i^{W-W} & Z_i^{W-PO} \\ Z_i^{PO-S} & Z_i^{PO-W} & C_i^{PO-PO} \end{bmatrix}\begin{bmatrix} P_{j-i}^S \\ P_{j-i}^W \\ P_{j-i}^{PO} \end{bmatrix} (13)$$

where the matrix elements and vectors are given by

$$Z_{i,mn}^{\zeta-v} = \left\langle \mathbf{f}_m^\zeta\left(\mathbf{r}\right), \int\limits_{S'}\frac{\mathbf{f}_n^v\left(\mathbf{r}'\right)}{R(c\Delta t)^2}T''\left(i-R/(c\Delta t)\right)dS' \right.$$

$$\left. -\nabla\int\limits_{S'}\frac{\nabla'\cdot\mathbf{f}_n^v\left(\mathbf{r}'\right)}{R}T\left(i-R/(c\Delta t)\right)dS' \right\rangle, \quad (14)$$

$$Z_{i,mn}^{\zeta-PO} = \left\langle \mathbf{f}_m^{\zeta}(\mathbf{r}), \int\limits_{S'} \frac{\mathbf{f}_n^{PO}(\mathbf{r}')}{R(c\Delta t)^2} T''(i - R/(c\Delta t)) \, dS' \right.$$

$$\left. -\nabla \int\limits_{S'} \frac{\nabla' \cdot \mathbf{f}_n^{PO}(\mathbf{r}')}{R} T(i - R/(c\Delta t)) \, dS' \right\rangle, \tag{15}$$

$$Z_{i,mn}^{PO-\upsilon} = \left\langle \mathbf{f}_m^{PO}(\mathbf{r}), \int\limits_{S'} \frac{\hat{\mathbf{n}} \times \hat{\mathbf{R}} \times \mathbf{f}_n^{\upsilon}(\mathbf{r}')}{R^2(c\Delta t)} T'(i - R/(c\Delta t)) \, dS' \right.$$

$$\left. + \int\limits_{S'} \frac{\hat{\mathbf{n}} \times \hat{\mathbf{R}} \times \mathbf{f}_n^{\upsilon}(\mathbf{r}')}{R(c\Delta t)^2} T''(i - R/(c\Delta t)) \, dS' \right\rangle, \tag{16}$$

$$C_i^{PO-PO} = \left\langle \mathbf{f}_m^{PO}(\mathbf{r}), \frac{2\pi}{c\Delta t} T'(i) \mathbf{f}_n^{PO}(\mathbf{r}') \right\rangle, \tag{17}$$

$$V_{j,m}^{\zeta} = \left\langle \mathbf{f}_m^{\zeta}(\mathbf{r}), \mathbf{E}^i(\mathbf{r}, t) \right\rangle \Big|_{t=t_j}, \tag{18}$$

$$V_{j,m}^{PO} = \left\langle \mathbf{f}_m^{PO}(\mathbf{r}), \hat{\mathbf{n}} \times \eta \mathbf{H}^i(\mathbf{r}, t) \right\rangle \Big|_{t=t_j}, \tag{19}$$

$$L = \text{Int}(R_{\max}/(c\Delta t) + 3), \tag{20}$$

and $< \cdot >$ is an inner product operator. $\text{Int}(\cdot)$ is an integration value operator. ζ and $\upsilon = S$ and W, respectively. $Z_i^{\zeta-\upsilon}$, $Z_i^{\zeta-PO}$, $Z_i^{PO-\upsilon}$ and C_i^{PO-PO} represent the multiple interactions among different TDIE and TDPO regions, while V_j^{ζ} and V_j^{PO} are the incident source vectors in the TDIE and TDPO regions, respectively. $R = |r - r'|$ represents the distance between an arbitrary observation point r and the source one r'. Δt is the time step, and $\tau = t - R/c$. The unknown current coefficient vector P_j in (13) can be computed from the known P_{j-i} and the incident source vector V_j.

In comparison with the pure TDIE method, the reduction in complexity of the hybrid TDIE-TDPO method is evident as mutual interactions between the TDPO regions are excluded. Therefore, we can eliminate the large matrix in TDPO region Z_i^{PO-PO} to C_i^{PO-PO}, with much memory and computational time saved. We introduce $\beta = N^{IE}/(N^{IE}+N^{PO})$, so the computational complexity of interaction in the same TDIE region scales as $O(\beta^2(N^{IE} + N^{PO})^2)$. While the computational complexity of interaction between the TDIE and TDPO regions is $O(\beta(1-\beta)(N^{IE} + N^{PO})^2)$. For the N_t time steps, the total computational complexity of the hybrid TDIE-TDPO method is $O(\beta N_t(N^{IE}+N^{PO})^2)$, and it is $O(N_t(N^{IE}+N^{PO})^2)$ for the pure TDIE

method. Therefore, it will be reduced drastically if the parameter β is very small, i.e., the TDIE region is electrically small.

3. NUMERICAL RESULTS AND DISCUSSION

According to the above numerical formulation, one hybrid algorithm is developed for accurately capturing EMP responses of several wire and surface structures. Here, we use a temporal pulse with a modulated Gaussian shape as an excitation, and it is given by

$$\mathbf{E}^i\left(\mathbf{r}, t\right) = \mathbf{u}_i E_0 \frac{4}{T\sqrt{\pi}} e^{-\gamma^2} \cos\left(2\pi f_0 t\right), \tag{21}$$

$$\mathbf{H}^i\left(r, t\right) = \frac{1}{\eta} \mathbf{k} \times \mathbf{E}^i\left(\mathbf{r}, t\right), \tag{22}$$

$$\gamma = \frac{4}{T}\left(ct - ct_0 - \mathbf{r}\cdot\mathbf{k}\right), \tag{23}$$

where $\mathbf{u}_i$ is the unit vector that defines the polarization of the incoming plane wave, E_0 is the amplitude of the incoming wave, T controls the width of the pulse, f_0 is the central frequency of the pulse, t_0 is the time delay, and $\mathbf{k}$ is the unit wave vector. Several numerical examples are given below to demonstrate the capability of our proposed hybrid method for capturing transient electromagnetic responses of some wire and surface structures, respectively.

Example 1: we at first consider a log periodic antenna (LPDA) placed near a square PEC plate, as shown in Fig. 2, both antenna and plate are illuminated by an EMP.
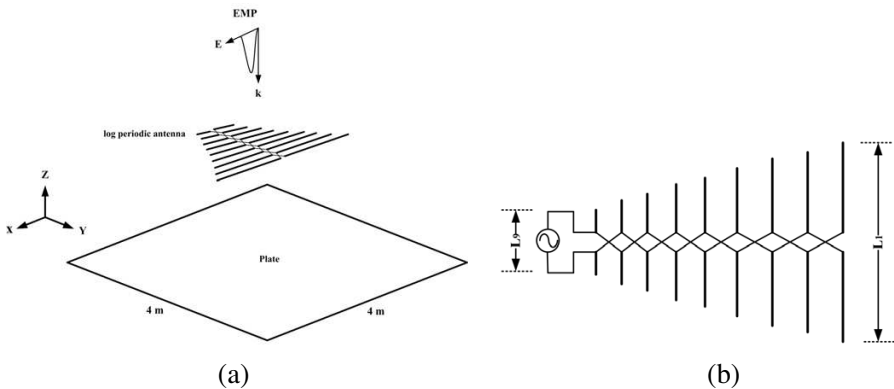

Figure 2. A log periodic antenna and a PEC plate are illuminated by an EMP at the same time. (a) 3-D and (b) top views of the LPDA, respectively.

In Fig. 2, the log periodic antenna consists of nine dipoles, the lengths of the longest and the shortest ones are chosen to be 0.345 m and 0.172 m, respectively. The structure parameters $\tau = 0.917$ and $\sigma = 0.07$, the width of the PEC plate is 4 m, and the distance between the log periodic antenna and the PEC plate is 1.0 m. One delta-gap source is used to feed the antenna [30–32], the feed point is shown in Fig. 2(b) and the source is chosen to be a modulated Gaussian pulse. The incident EMP with the polarization along the direction of $+x$, characterized by $T = 26.67$ ns, $ct_0 = 33.33$ ns, $E_0 = 20.0$ kV/m, and $f_0 = 200$ MHz, propagates along the $-z$ axis. The extension of the TDIE region in our calculation is not only on the wire, but also on one part of PEC plate, and the remaining part of the plate is the TDPO one. Fig. 3(a) shows the transient current response captured at the feed point of the shortest dipole, with the case of no-EMP incidence also given for comparison, and Fig. 3(b) shows the comparison of the backward scattered EMP field in the far zone obtained by TDIE-TDPO-MOT and TDIE-MOT methods, respectively, and it is evident that good agreement is obtained between them. The computational time used by the TDIE-MOT method is about 10.55 minutes, while for the TDIE-TDPO-MOT one, it is only about 2.33 minutes.

Example 2: Fig. 4(a) shows a log periodic antenna placed near a partial sphere, with its transient current response recorded at the feed point of the shortest dipole plotted in Fig. 4(b). While Fig. 4(c) shows the backward scattered EMP field of both objects in the far zone.

In Fig. 4(a), the sphere radius is chosen to be 3.0 m, its bottom radius is given by 2.14 m, its height is set to be 0.9 m, and the
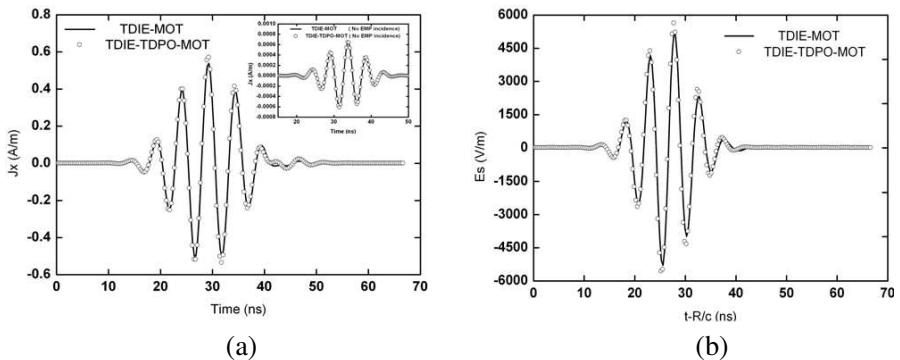

Figure 3. (a) Transient current recorded at the feed point of the shortest dipole. (b) The backward scattered EMP field of both objects in the far zone.
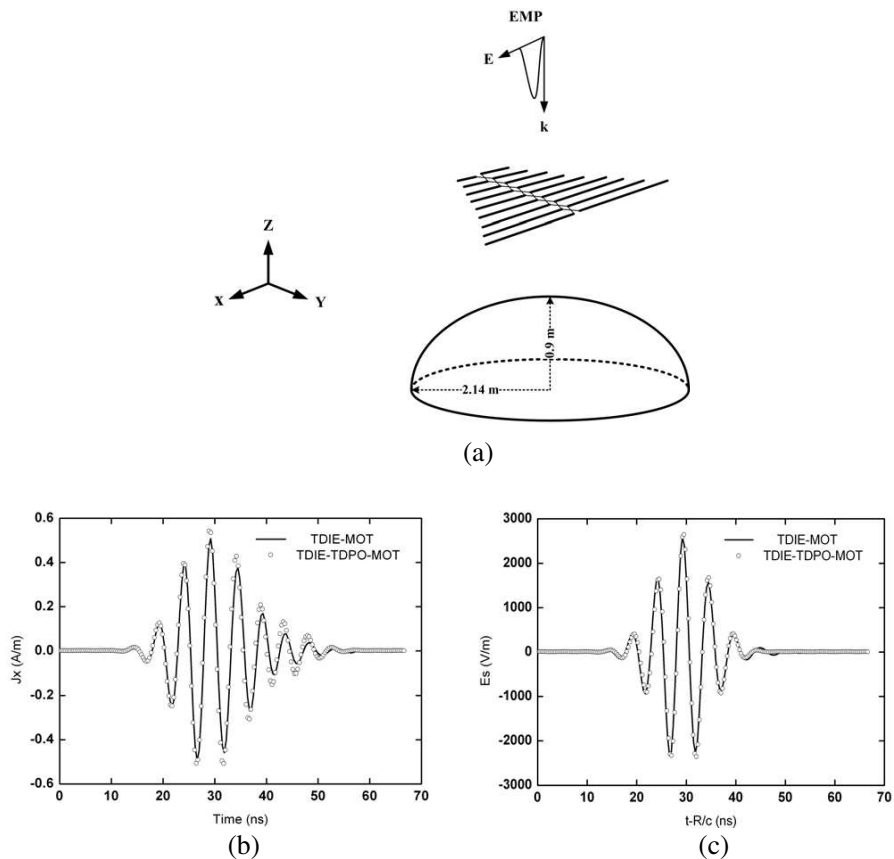
Figure 4. (a) A log periodic antenna is placed near a partial sphere. (b) Transient current recorded at the feed point of the shortest dipole. (c) The backward scattered EMP field of both objects in the far zone.

distance between the antenna and the object is 1.0 m. The geometrical parameters of the antenna are the same as the one in Fig. 2, and the incident EMP also takes the same form as above. Again, we have compared the time taken by both TDIE-MOT and TDIE-TDPO-MOT methods, and they are about 6.67 and 2.13 minutes, respectively.

Example 3: we further consider the case of a log periodic antenna near three parallel cylinders with the same length, as shown in Fig. 5.

In Fig. 5, the radius and the length of each cylinder are chosen to be 0.3 and 2.0 m, respectively, the distance between the central cylinder and the antenna is 1.2 m, and the distance between two adjacent cylinders is given by 1.0 m, respectively. The geometrical parameters
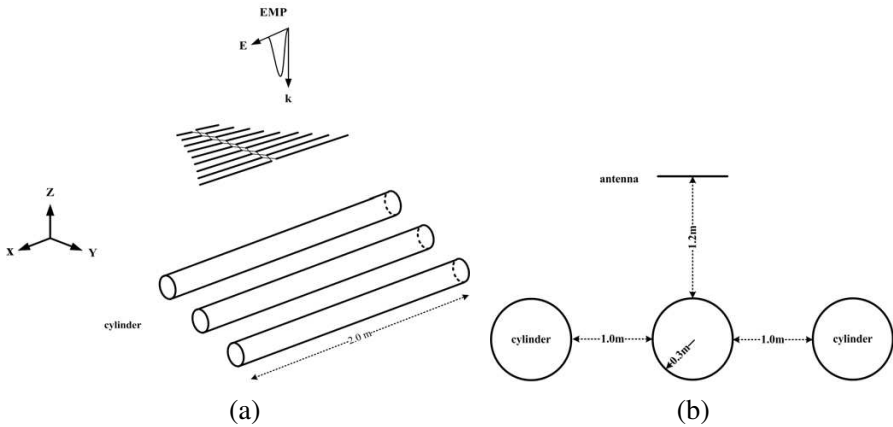
Figure 5. A log periodic antenna is placed near three finite cylinders illuminated by an EMP at the same time. (a) 3-D and (b) cross-sectional views, respectively.
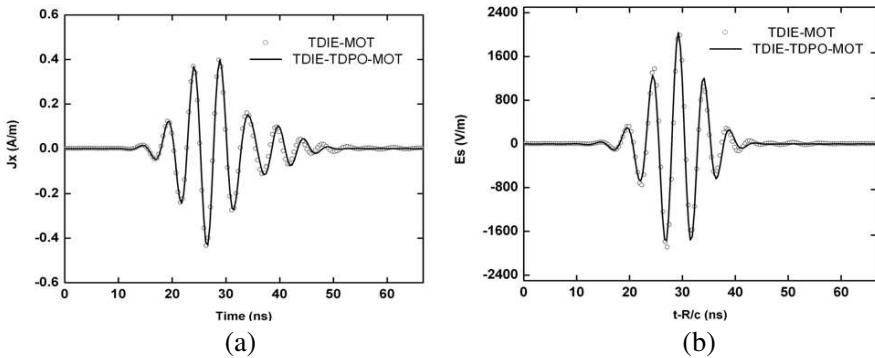

Figure 6. (a) Transient current recorded at the feed point of the shortest dipole. (b) The backward scattered EMP field of both objects in the far zone.

of the antenna are the same as the one used above. Figs. 6(a) and (b) show the transient current response recorded at the feed point of the shortest dipole and the backward scattered EMP field of both objects in the far zone, respectively. Here, the computational time used by the TDIE-MOT method is about 11.08 minutes, while for the TDIE-TDPO-MOT one, it is only about 3.25 minutes.

Example 4: Further, we consider the case of a log periodic antenna placed behind three finite cylinders, as shown in Fig. 7, and both of
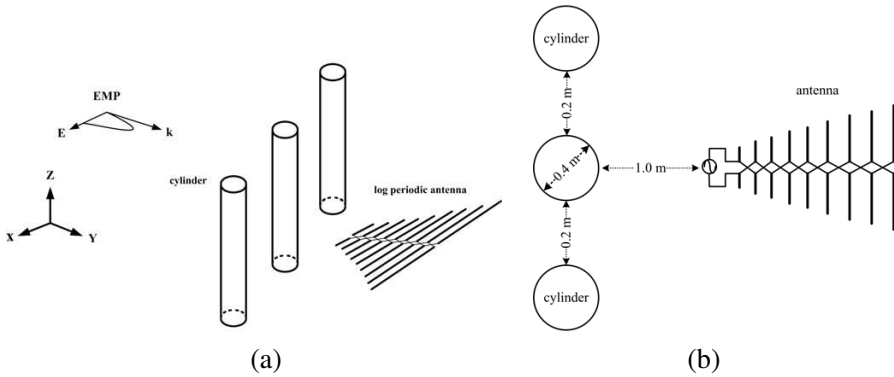
Figure 7. A log periodic antenna is placed behind three finite cylinders. (a) 3-D and (b) cross-sectional views.
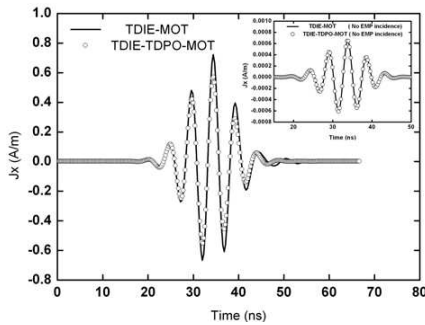

Figure 8. Transient current recorded at the feed point of the shortest dipole.
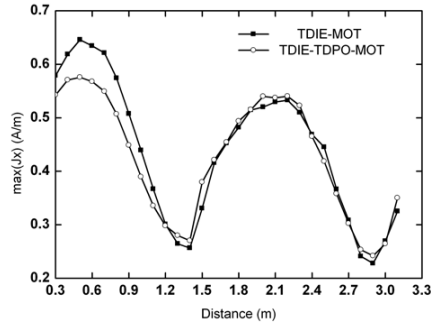
Figure 9. The maximum surface current recorded at the central point of the shortest dipole as a function of the distance between the antenna and the three cylinders.

them are also illuminated by an EMP. The radius and the length of each cylinder are given by $0.2\,\mathrm{m}$ and $2.0\,\mathrm{m}$, the distance between two adjacent cylinders is $0.2\,\mathrm{m}$, and the distance between the antenna and the central cylinders is $1.0\,\mathrm{m}$. The geometrical parameters of antenna are the same as the one in Fig. 2. The incident EMP propagates along the $+y$ axis, with the polarization along the direction of $+x$, characterized by $T = 26.67\,\mathrm{ns}$, $ct_0 = 33.33\,\mathrm{ns}$, $E_0 = 20.0\,\mathrm{kV/m}$, and $f_0 = 200\,\mathrm{MHz}$.

Figure 8 shows the transient current recorded at the feed point

of the shortest dipole, and the case of no EMP incidence is also given for comparison. Obviously, the current response obtained by TDIE-TDPO-MOT method agrees well with that of TDIE-MOT one, but both computational complexity and time in the former calculation are reduced significantly.

Further, as the distance between antenna and three cylinders in Fig. 7 is varied from 0.3 to 3.1 m, the captured maximum surface current at the feed point of the shortest dipole is plotted in Fig. 9.

It is evident that proximity effect between the antenna and the three cylinders on the maximum surface current at the central point of the shortest dipole is evident, which does not change monotonously with increasing the distance. The central frequency of the incident
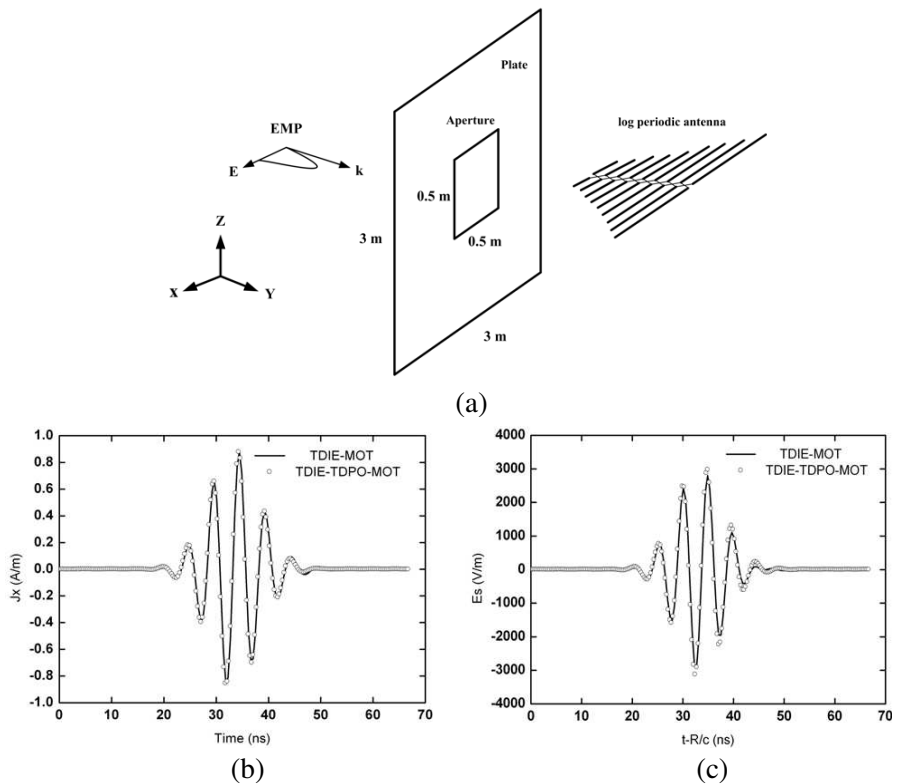

(a)

(b)

(c)

Figure 10. (a) A log periodic antenna placed behind of a PEC plate with an aperture. (b) Transient current response recorded at the central point of the shortest dipole. (c) The backward scattered EMP field of both objects in the far zone.

EMP is set to be 200 MHz, so the distance is comparable with single wavelength. On the other hand, we would like to indicate that as the distance is decreased from 1.2 to 0.3 m, the antenna is in the shadow region of three cylinders, and under such circumstances, the accuracy of TDIE-TDPO-MOT method is reduced in comparison with that of TDIE-MOT one.

Example 5: Fig. 10(a) shows a log periodic antenna placed behind of a PEC plate with an aperture, and its transient EMP responses are plotted in Figs. 10(b) and (c), respectively.

In Fig. 10(a), the width of the PEC plate is chosen to be 3.0 m, the aperture size is given by 0.5 m × 0.5 m, and the distance between the antenna and the PEC plate is given by 1.0 m. The incident high-power EMP propagates along the $+y$ axis, with its polarization along the direction of $+x$, characterized by $E_0 = 20.0\,\text{kV/m}$, $T = 26.67\,\text{ns}$, $ct_0 = 33.33\,\text{ns}$, and $f_0 = 200\,\text{MHz}$. It is also demonstrated that the EMP responses predicted by both TDIE-TDPO-MOT and TDIE-MOT methods agree well each other, but the computational time is very different between them.

As all the geometrical parameters in Fig. 10(a) are not changed, but the distance between the antenna and the PEC plate is varied from 0.7 to 5.0 m, Fig. 11 shows the maximum surface currents recorded at the central point of the shortest dipole for $f_0 = 200$ and 300 MHz, respectively. It is obvious that the maximum current changes periodically as the distance varies.

Finally, we choose the aperture size on the PEC plate as (a) 0.5 m × 0.5 m and (b) 0.125 m × 2.0 m (slot), respectively, while the EMP parameters are the same as those in Fig. 10(a), and the distance
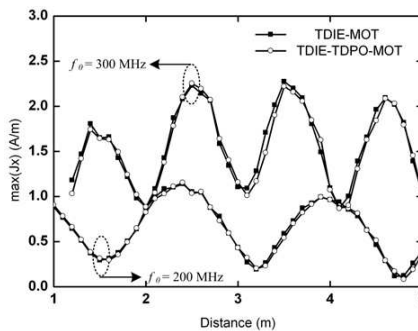

Figure 11. The maximum surface current recorded at the central point of the shortest dipole as a function of the distance between the antenna and the PEC plate.
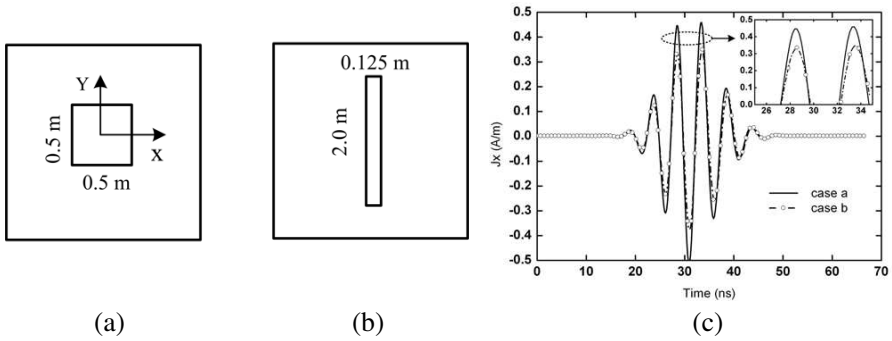
Figure 12. The aperture size on the PEC plate is (a) 0.5 m × 0.5 m and (b) 0.125 m × 2.0 m (slot). (c) Transient current responses recorded at the central point of the shortest dipole.

is given by $d = 0.3$ m. Fig. 12 shows the comparison of the transient currents recorded at the central point of the shortest dipole for two cases.

In Fig. 12, two apertures on the PEC plate have the same area. It is observed that the transient current response in Case (a) is stronger than that of Case (b), which indicates that the slot orientation on the PEC plate does have certain effect on the transient current response of the antenna. Of course, after some numerical experiments, we can suppress the current response by choosing an appropriate slot geometry or its orientation.

4. CONCLUSION

In this paper, an efficient hybrid method, based on time-domain integral equation (TDIE) and time-domain physical optics (TDPO), is proposed for studying electromagnetic responses of several groups of wire and surface structures illuminated by an electromagnetic pulse (EMP), respectively. Two triangular-type basis functions are used to represent the currents on the PEC wires and PEC surfaces, respectively. In comparison with the full TDIE-MOT method, computational complexity can be reduced drastically using our developed TDIE-TDPO-MOT method, and computational accuracy is still maintained. The above numerical examples demonstrate that it can be employed to predict electromagnetic pulse responses of various multi-scale perfectly conducting objects.

ACKNOWLEDGMENT

REFERENCES

1. Jung, B. H., T. K. Sarkar, and Y.-S. Chung, "A survey of various frequency domain integral equations for the analysis of scattering from three-dimensional dielectric objects," *Progress In Electromagnetics Research*, Vol. 36, 193–246, 2002.

2. Fikioris, G. and C. A. Valagiannopoulos, "Input admittances arising from explicit solutions to integral equations for infinite-length dipole antennas," *Progress In Electromagnetics Research*, Vol. 55, 285–306, 2005.

3. Hanninen, I., M. Taskinen, and J. Sarvas, "Singularity subtraction integral formulae for surface integral equations with RWG, rooftop and hybrid basis functions," *Progress In Electromagnetics Research*, Vol. 63, 243–278, 2006.

4. Wen, G., "New magnetic field integral equation for antenna system," *Progress In Electromagnetics Research*, Vol. 63, 153–170, 2006.

5. Zhang, G. H., M. Xia, and C. H. Chan, "Time domain integral equation approach for analysis of transient responses by metallic-dielectric composite bodies," *Progress In Electromagnetics Research*, Vol. 87, 1–14, 2008.

6. Zhang, G. H., M. Xia, and X. M. Jiang, "Transient analysis of wire structures using time domain integral equation method with exact matrix elements," *Progress In Electromagnetics Research*, Vol. 92, 281–298, 2009.

7. Qin, S. T., S. X. Gong, R. Wang, and L. X. Guo, "A TDIE/TDPO hybrid method for the analysis of TM transient scattering from two-dimensional combinative conducting cylinders," *Progress In Electromagnetics Research*, Vol. 102, 181–195, 2010.

8. Cui, Z.-W., Y.-P. Han, and M.-L. Li, "Solution of CFIE-JMCFIE using parallel MoM for scattering by dielectrically coated conducting bodies," *Journal of Electromagnetic Waves and Applications*, Vol. 25, No. 2–3, 211–222, 2011.

9. Ashraf, M. A. and A. A. Rizvi, "Electromagnetic scattering from a random cylinder by moments method," *Journal of

Electromagnetic Waves and Applications, Vol. 25, No. 4, 467–480, 2011.

10. Lai, B., H. B. Yuan, and C. H. Liang, "Analysis of nurbs surfaces modeled geometries with higher-order MoM based aim," *Journal of Electromagnetic Waves and Applications*, Vol. 25, No. 5–6, 683–691, 2011.

11. Rao, S. M. and T. K. Sarkar, "An alternative version of the time domain electric field integral equation for arbitrarily shaped conductors," *IEEE Trans. Antennas Propag.*, Vol. 41, No. 6, 831–834, 1993.

12. Manara, G., A. Monorchio, and R. Reggiannini, "A space-time discretization criterion for a stable time-marching solution of the electric field integral equation," *IEEE Trans. Antennas Propag.*, Vol. 45, No. 3, 527–532, 1997.

13. Bluck, M. J. and S. P. Walker, "Time-domain BIE analysis of large three dimensional electromagnetic scattering problems," *IEEE Trans. Antennas Propag.*, Vol. 45, No. 5, 894–901, 1997.

14. Weile, D. S., G. Pisharody, N. W. Chen, B. Shanker, and E. Michielssen, "A novel scheme for the solution of the time-domain integral equations of electromagnetics," *IEEE Trans. Antennas Propag.*, Vol. 52, No. 1, 283–295, 2004.

15. Wang, X., R. A. Wildman, D. S. Weile, and P. Monk, "A finite difference delay modelling approach to the discretization of the time domain integral equations of electromagnetic," *IEEE Trans. Antennas Propag.*, Vol. 56, No. 8, Part 1, 2442–2452, 2008.

16. Andriulli, F. P., K. Cools, F. Olyslager, and E. Michielssen, "Time domain calderón identities and their application to the integral equation analysis of scattering by PEC objects Part II: Stability," *IEEE Trans. Antennas Propag.*, Vol. 57, No. 8, 2365–2375, 2009.

17. Xue, M. F. and W. Y. Yin, "Wideband pulse responses of fractal monopole antennas under the impact of an EMP," *IEEE Trans. Electromagn. Compat.*, Vol. 52, No. 1, 98–107, 2010.

18. Zhu, M. D., X. L. Zhou, and W. Y. Yin, "An adaptive marching-on-in-order method with FFT-based blocking scheme," *IEEE Antennas Wireless Propagation Lett.*, Vol. 9, 436–439, 2010.

19. Xia, M. Y., G. H. Zhang, and G. L. Dai, "Stable solution of time domain integral equation methods using quadratic B-spline temporal basis functions," *International Journal of Computational Mathematics*, Vol. 25, No. 3, 374–384, 2007.

20. Rao, S. M. and D. R. Wilton, "Transient scattering by conducting surfaces of arbitrary shape," *IEEE Trans. Antennas Propag.*,

Vol. 39, No. 1, 56–61, 1991.

21. Walker, S. P. and M. J. Vartiainen, "Hybridization of curvilinear time-domain integral equation and time-domain optical methods for electromagnetic scattering analysis," *IEEE Trans. Antennas Propag.*, Vol. 46, No. 3, 318–324, 1998.

22. Kobidze, G., B. Shanker, and E. Michielssen, "Hybrid PO-PWTD scheme for analysing of scattering from electrically large PEC objects," *IEEE Antennas Propagation Society Int. Symp.*, Vol. 3, 547–555, 2003.

23. Sun, E.-Y. and W. V. T. Rusch, "Time-domain physical-optics," *IEEE Trans. Antennas Propag.*, Vol. 42, 9–15, Jan. 1994.

24. Reng, M., D. M. Zhou, Y. Li, and J. G. He, "Coupled TDIE-PO method for transient scattering from electrically large conducting objects," *Electronics Lett.*, Vol. 44, No. 4, 258–260, 2008.

25. Ling, J., S. Gong, S. Qin, W. Wang, and Y. Zhang, "Wide-band analysis of on-platform antenna using MoM-PO combined with Maehly approximation," *Journal of Electromagnetic Waves and Applications*, Vol. 24, No. 4, 475–484, 2010.

26. Su, J., X. Xu, and B. Hu, "Hybrid PMM-MoM method for the analysis of finite periodic sytuctures," *Journal of Electromagnetic Waves and Applications*, Vol. 25, No. 2–3, 267–282, 2011.

27. Rao, S. M., D. R. Wilton, and A. W. Glisson, "Electromagnetic scattering by surfaces of arbitrary shape," *IEEE Trans. Antennas Propag.*, Vol. 30, No. 3, 409–418, 1982.

28. Ji, Z., T. K. Sarkar, B. H. Jung, Y. S. Chung, M. Salazar-Palma, and M. Yuan, "A stable solution of time domain electric field integral equation for thin-wire antennas using the Laguerre polynomials," *IEEE Trans. Antennas Propag.*, Vol. 52, No. 10, 2641–2649, 2004.

29. Hwu, S. U., D. R. Wilton, and S. M. Rao, "Electromagnetic scattering and radiation by arbitrary wire/surface configurations," *IEEE AP-S Dig.*, Vol. 6, No. 2, 890–893, 1998.

30. Junker, G. P., A. A. Kishk, and A. W. Glisson, "A novel delta gap source model for center fed cylindrical dipoles," *IEEE Trans. Antennas Propag.*, Vol. 43, No. 5, 537–540, 1995.

31. Makarov, S., "MoM antenna simulation with Matlab: RWG basis functions," *IEEE Trans. Antennas Propag.*, Vol. 43, No. 5, 100–107, 2001.

32. Aygün, K., B. Shanker, and A. A. Ergin, "A two-level plane wave time-domain algorithm for fast analysis of EMC/EMI problems," *IEEE Trans. Electromagn. Compat.*, Vol. 44, No. 1, 152–164, 2002.